Inorg. Chem. **1991**, *30*, 3276-3280

Contribution from the Department of Chemistry,
University of South Carolina, Columbia, South Carolina 29208

Molecular Structures, Stabilities, and Electronic States of the Planar Rings $S_3N_2^+$ and $S_3N_2^{2+}$

Benjamin M. Gimarc* and D. Scott Warren

Received February 4, 1991

Among planar inorganic aromatic rings, the largest class consists of the sulfur-nitrogen rings: S_2N_2, $S_3N_2^{2+}$, $S_3N_2^+$, $S_3N_3^-$, $S_4N_3^+$, $S_4N_4^{2+}$, and $S_5N_5^+$. Of these, $S_3N_2^+$ and $S_3N_2^{2+}$ are perhaps the most curious. ESR studies confirm that $S_3N_2^+$ is a radical cation with an electronic state $^2A_2$ and seven π electrons. $S_3N_2^{2+}$ is a six-π-electron system. Although the dication has been prepared as a solid, it decomposes in solution to SN^+ and SNS^+. Our geometry-optimized ab initio SCF MO calculations for $S_3N_2^+$ at the STO-3G* and 6-31G* levels give a structure that agrees with experiment. Similar calculations provide bond distances and angles for $S_3N_2^{2+}$, the detailed structure of which is unknown. We can correlate the MO's of $S_3N_2^{2+}$ with those of its decomposition products and show that the decomposition of $S_3N_2^+$, known to be quite stable, is not allowed by symmetry. We report total energies of $^2A_2$ and $^2B_1$ states of $S_3N_2^+$, discuss possible electronic states and molecular structures for the unknown neutral S_3N_2, and rationalize results using qualitative MO theory.

Introduction

The sulfur-nitrogen heterocycles form the largest class of planar inorganic aromatic rings.[1-5] This group consists of S_2N_2, $S_3N_2^{2+}$, $S_3N_2^+$, $S_3N_3^-$, $S_4N_3^+$, $S_4N_4^{2+}$, and $S_5N_5^+$. Two of the most curious members of the class are $S_3N_2^+$ (**1**)[6-11] and $S_3N_2^{2+}$ (**2**),[12] Figure 1. The planar monocycle **1** is a radical cation. Its ESR spectrum has been observed in crystal, powder, and solution.[13-16] The radical cation **1** is known to exist in certain crystals as an isolated monomer but it more often occurs as the very loosely associated dimer **3** with the two five-membered rings in parallel planes and their S-S edges separated by about 3 Å. Structural parameters shown for **1** in Figure 1 are averages of X-ray results from several sources.[10] A detailed structure of **2** has not yet been reported.

The rule for counting π electrons in planar sulfur-nitrogen rings calls for summing one electron from each nitrogen and two electrons from each sulfur and adding or subtracting electrons to match the overall charge if the species is an ion.[1,17] This counting procedure shows **1** to be a seven-π-electron system while the dication **2** has six π electrons. Although **2** has been observed in the solid by vibrational spectroscopy, this ring readily dissociates in liquid SO_2 solution according to eq 1.

$$\underset{\mathbf{2}}{S_3N_2^{2+}} \rightarrow \underset{\mathbf{4}}{NS^+} + \underset{\mathbf{5}}{SNS^+} \qquad (1)$$

The decomposition products **4** and **5** are themselves well-known. NS^+ is isoelectronic with N_2 and P_2; SNS^+ is a linear, symmetric ion isoelectronic with CO_2 and CS_2. Experimental bond distances for **4** and **5** appear in Figure 1. The 1.440-Å N≡S triple-bond distance in **4** comes from an analysis of vibrational bands observed by photoelectron spectroscopy.[18] The distance reported from a crystallographic study is somewhat shorter, 1.42 Å.[19] The value 1.470 Å for the N=S double bond in **5** is an average of distances from several X-ray structures involving different counterions.[20-22] The molecule H_2NSH (**6**) contains a NS single bond. The structure of H_2NSH has been determined by microwave spectroscopy, which shows that cis and trans conformers have very similar energies and SN bond distances of 1.705 and 1.719 Å, respectively.[23] The experimental data show that the SN bond distances in the $S_3N_2^+$ ring fall between those for standard SN single and double bonds as expected for delocalized bonding in a planar aromatic system. In this paper, we report a theoretical study of the electronic and molecular structures of the known heteroatomic rings $S_3N_2^+$ and $S_3N_2^{2+}$ and the hypothetical neutral species S_3N_2 in various electronic states as well as the structures of a number of known and hypothetical diatomic and triatomic sulfur-nitrogen fragments. We employ all levels of molecular orbital theory from the qualitative model[24] to geometry-optimized ab initio SCF MO calculations in order to rationalize the stabilities of different electronic states, to correlate bond distance differences in various states and species with the nodal properties of the MO's involved, and to compare the stabilities of the rings with those of separated diatomic and triatomic fragments.

π MO's

The π MO's of $S_3N_2^+$ and $S_3N_2^{2+}$ are related to those of the homoatomic rings $C_5H_5^-$ and P_5^-. Both sulfur and nitrogen are more electronegative than carbon and phosphorus and therefore the π energy levels of the heterocycles are displaced to lower energies relative to those of $C_5H_5^-$ or P_5^-, as suggested in Figure 2. The degeneracies of the upper two sets of homocyclic π MO's (1e″ and 2e″) are removed in the lower symmetry (C_{2v}) heterocycles. But because of the diagonal relationship between S and N in the periodic table, simple Hückel Coulomb integral parameters for S and N are similar, as are extended Hückel Coulomb integrals (valence-state ionization energies for S and N), and therefore the actual splittings of degenerate e″ levels turn out to be small, particularly between the two MO's, $2a_2$ and $3b_1$, that come from the highest level 2e″.[25]

---

(1) Banister, A. J. *Nature, Phys. Sci.* **1972**, *237*, 92.
(2) Roesky, H. W. *Angew. Chem., Int. Ed. Engl.* **1979**, *18*, 91.
(3) Gimarc, B. M.; Trinajstic, N. *Pure Appl. Chem.* **1980**, *52*, 1443.
(4) Chivers, T. *Chem. Rev.* **1985**, *85*, 341.
(5) Oakley, R. T. *Prog. Inorg. Chem.* **1988**, *36*, 299.
(6) Banister, A. J.; Clarke, H. G.; Rayment, I.; Shearer, H. M. M. *Inorg. Nucl. Chem. Lett.* **1974**, *10*, 647.
(7) Gillespie, R. J.; Ireland, P. R.; Vekris, J. E. *Can. J. Chem.* **1975**, *53*, 3147.
(8) Roesky, H. W.; Hamza, A. *Angew. Chem., Int. Ed. Engl.* **1976**, *15*, 226.
(9) Krebs, B.; Henkel, G.; Pohl, S.; Roesky, H. W. *Chem. Ber.* **1980**, *113*, 226.
(10) Gillespie, R. J.; Kent, J. P.; Sawyer, J. F. *Inorg. Chem.* **1981**, *20*, 3784.
(11) Thewalt, U.; Burger, M. *Z. Naturforsch.* **1981**, *36B*, 293.
(12) Passmore, J.; Schriver, M. J. *Inorg. Chem.* **1988**, *27*, 2749.
(13) Fairhurst, S. A.; Preston, K. F.; Sutcliffe, L. H. *Can. J. Chem.* **1984**, *62*, 1124.
(14) Fairhurst, S. A.; Johnson, K. M.; Sutcliffe, L. H.; Preston, K. F.; Banister, A. J.; Hauptman, Z. V.; Passmore, J. *J. Chem. Soc., Dalton Trans.* **1986**, 1465.
(15) Preston, K. F.; Charland, J.-P.; Sutcliffe, L. H. *Can. J. Chem.* **1988**, *66*, 1299.
(16) Awere, E.; Passmore, J.; Preston, K. F.; Suttcliffe, L. H. *Can. J. Chem.* **1988**, *66*, 1766.
(17) Gimarc, B. M.; Juric, A.; Trinajstic, N. *Inorg. Chim. Acta* **1985**, *102*, 105.
(18) Dyke, J. M.; Morris, A.; Trickle, I. R. *J. Chem. Soc., Faraday Trans.* **1977**, *73*, 147.
(19) Clegg, W.; Glemser, O.; Harms, K.; Hartmann, G.; Mews, R.; Noltemeyer, M.; Sheldrick, G. M. *Acta Crystallogr.* **1981**, *B37*, 548.
(20) Faggiani, R.; Gillespie, R. J.; Lock, C. J. L.; Tyrer, J. D. *Inorg. Chem.* **1978**, *17*, 2975.
(21) Thewalt, U.; Berhalter, K.; Müller, P. *Acta Crystallogr.* **1982**, *B38*, 1280.
(22) Johnson, J. P.; Passmore, J.; White, P. S.; Banister, A. J.; Kendrick, A. G. *Acta Crystallogr.* **1987**, *43C*, 1651.
(23) Lovas, F. J.; Suenram, R. D.; Stevens, W. J. *J. Mol. Spectrosc.* **1983**, *100*, 316.
(24) Gimarc, B. M. *Molecular Structure and Bonding*; Academic Press: New York, 1979.

0020-1669/91/1330-3276$02.50/0

Table I. Total Energies for Sulfur–Nitrogen Species at Different Levels of Theory[a]

species	E_{total}, hartrees STO-3G*	6-31G*	6-31G*/MP2	$E_{relative}$ for 6-31G*/MP2, kcal/mol
$S_3N_2^{2+}(^1A_1)$	−1286.545 87	−1300.504 03	−1301.231 31	
$S_3N_2^{+}(^2A_2)$	−1286.994 01	−1301.026 62	−1301.717 13	0
$S_3N_2^{+}(^2B_1)$	−1286.990 57	−1301.005 66	−1301.669 38	+30.0
$S_3N_2(^1A_1)(2a_2)^2$	−1287.118 35	−1301.273 06	−1302.000 99	0
$S_3N_2(^3B_2)$	−1287.169 72	−1301.309 95	−1301.970 22	+19.3
$S_3N_2(^1A_1)(3b_1)^2$	−1287.046 43	−1301.181 21	−1301.952 79	+30.2
SN^+	−446.665 68	−451.565 53	−451.862 31	
SN	−446.919 81	−451.898 39	−452.123 62	
SNS^+	−839.915 15	−849.090 24	−849.560 30	
SNS	−840.081 75	−849.380 65	−849.797 94	
NNS	−500.615 72	−506.372 86	−506.813 43	0
NSN	−500.525 94	−506.164 09	−506.677 91	85.1
H_2NSH(trans)	−448.666 48	−453.674 69	−453.959 06	0
H_2NSH(cis)	−448.667 62	−453.673 84	−453.957 51	1.0
S_2^{2+}	−785.661 11	−794.046 21	−794.303 25	

[a] Optimizations required five-atom rings to be planar and triatomic chains to be linear. Distances and angles in H_2NSH were all optimized.

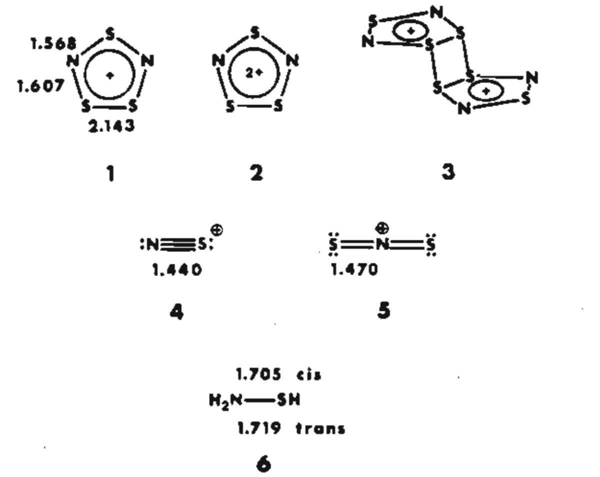

Figure 1. Sulfur–nitrogen heterocycles $S_3N_2^+$, $S_3N_2^{2+}$, $S_6N_4^{2+}$, the fragments NS^+ and SNS^+, and the molecule H_2NSH. Average experimental bond distances (Å) are shown.

ESR spectra of the seven-π-electron radical $S_3N_2^+$ (1) are consistent with an assignment of $^2A_2$ as the electronic state and a small or zero unpaired spin density on the unique sulfur as indicated by the nodal properties of the singly occupied MO of highest energy, $2a_2$, in Figure 2.[13–16] The dication 2 should be a closed-shell singlet state with six π electrons filling the levels $1b_1$, $1a_2$, and $2b_1$.

A comparison of simple Hückel energy levels for the planar sulfur–nitrogen rings reveals two curious features of the $S_3N_2^+$ levels and gives insight into the stabilities of various electronic states.[3] First, the singly occupied π level $2a_2$ has the highest energy of all the HOMO's in the known planar SN rings. Second, if the $2a_2$ level were empty, as it must be in the dication 2, then $2b_1$ of $S_3N_2^{2+}$ would be the lowest energy HOMO in the entire SN ring series. (Actually, $S_4N_4^{2+}$, another dication, has a HOMO of the same energy as $2b_1$.)

Since $2a_2$ is lower than $3b_1$, we expect the $^2A_2$ state of $S_3N_2^+$ to lie lower in energy than the $^2B_1$ state. For neutral S_3N_2, one might question where the extra electron goes since the $2a_2$, $3b_1$ splitting is small. If the extra electron pairs with the one already present in $2a_2$, higher electron–electron repulsions in the resulting singlet state $^1A_1$ with closed-shell configuration $(2a_2)^2$ might make this state higher in energy than if the second electron went into the vacant but only slightly higher $3b_1$ orbital to give the open-shell configuration $(2a_2)^1(3b_1)^1$ and the triplet state $^3B_2$.[26]

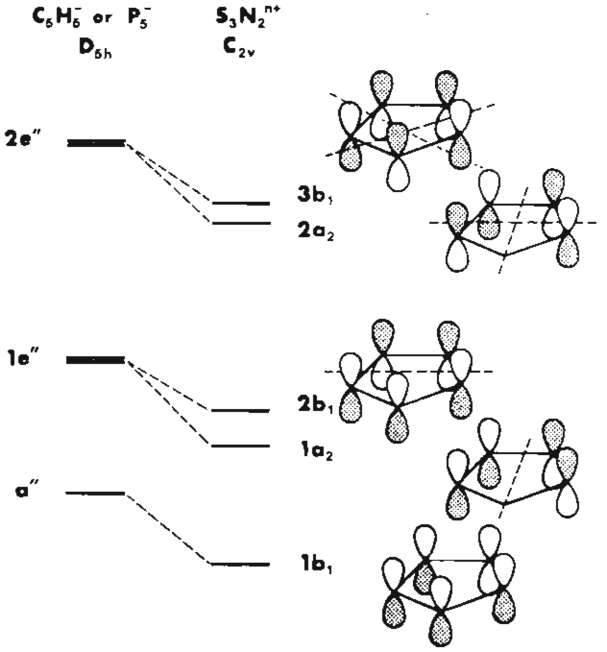

Figure 2. Relative π MO energies of the homoatomic ions $C_5H_5^-$ or P_5^- compared to those for the $S_3N_2^{n+}$ heterocycles. Qualitative AO composition diagrams for each MO indicate the nodal character of the MO.

Ab Initio Calculations

We have carried out geometry optimized ab initio SCF MO calculations for $S_3N_2^+$, $S_3N_2^{2+}$, S_3N_2, SN^+, SN, SNS^+, SNS, NSN, and NNS with STO-3G* and 6-31G* basis sets using the GAUSSIAN 86 program package.[27] The asterisk indicates that the basis sets have been augmented by d-type polarization functions, which experience shows are essential for an adequate description of structural details for compounds containing second-row atoms (in this case, sulfur).[28,29] At the suggestion of a reviewer, we have also included MP2 electron correlation corrections to the 6-31G* energies. Table I contains calculated total energies. Geometry optimizations were carried out subject to the constraints that the pentatomic rings remain planar and the triatomic chains stay linear. Although $S_3N_2^+$ is known to be planar from experiment and $S_3N_2^{2+}$ is

---

(25) A lengthy discussion of the basis for choosing simple Hückel heteroatom parameters for sulfur and nitrogen appears in ref 17. Since we wanted $2a_2$ to lie below $3b_1$ to match the energy order of extended Hückel and ab initio orbitals, we chose the nitrogen Coulomb integral to be deeper in energy than that for sulfur.

(26) Albright, T. A.; Burdett, J. K.; Whangbo, M.-H. *Orbital Interactions in Chemistry*; Wiley: New York, 1985; p 122.

(27) Frisch, M. J.; Binkley, J. S.; Schlegel, H. B.; Raghavachari, K.; Melius, C. F.; Martin, R. L.; Stewart, J. J. P.; Bobrowicz, F. W.; Rohlfing, C. M.; Kahn, L. R.; Defrees, D. J.; Seeger, R.; Whiteside, R. A.; Fox, D. J.; Fleuder, E. M.; Pople, J. A. *GAUSSIAN 86*; Carnegie Mellon Quantum Chemistry Publishing Unit: Pittsburgh, PA, 1984.

(28) Trinquier, G.; Daudey, J.-P.; Komiha, N. *J. Am. Chem. Soc.* **1985**, *107*, 7210.

(29) Raghavachari, K.; Haddon, R. C.; Binkley, J. S. *Chem. Phys. Lett.* **1985**, *122*, 219.

Table II. Bond Distances (Å) for Sulfur–Nitrogen Species Calculated at the 6-31G* Level (with STO-3G* Results in Parentheses)[a]

	calcd				exptl		
species	R(NS)[b]	R(NS)	R(SS)	R(NN)	R(NS)[b]	R(NS)	R(SS)
$S_3N_2^{2+}$ ($^1A_1$)	1.597	1.535	2.093				
	(1.619)	(1.572)	(2.016)				
$S_3N_2^+$ ($^2A_2$)	1.570	1.606	2.135		1.568	1.607	2.143
	(1.598)	(1.625)	(2.042)				
$S_3N_2^+$ ($^2B_1$)	1.688	1.597	2.000				
	(1.699)	(1.638)	(1.931)				
S_3N_2 ($^3B_2$)	1.677	1.632	2.120				
	(1.681)	(1.645)	(2.022)				
S_3N_2 ($^1A_1$)$(2a_2)^2$	1.514	1.701	2.173				
	(1.534)	(1.708)	(2.060)				
S_3N_2 ($^1A_1$)$(3b_1)^2$	1.763	1.534	1.954				
	(1.753)	(1.556)	(1.880)				
SN^+		1.397				1.440	
		(1.433)					
SN		1.556				1.496	
		(1.596)					
SNS^+		1.474				1.470	
		(1.482)					
SNS		1.529					
		(1.522)					
NNS		1.651		1.086			
		(1.562)		(1.159)			
NSN		1.419					
		(1.448)					
H_2NSH (cis)		1.696				1.705	
		(1.685)					
H_2NSH (trans)		1.710				1.719	
		(1.698)					
S_2^{2+}			1.719				
			(1.712)				

[a] Geometries were optimized by requiring five-atom rings to be planar and triatomic chains to be linear. Distances and angles in H_2NSH were all optimized. [b] Distance from nitrogen to the unique sulfur in the heterocycle.

presumed to be planar from isoelectronic analogy with $C_5H_5^-$ and P_5^-, the planarity of neutral S_3N_2 is more problematic. Nonetheless the vibrational frequencies calculated at the 6-31G* level for planar S_3N_2 ($^3B_2$) are all positive, although the calculated frequency of lowest energy is only about 50 cm^{-1}. Table II compares optimized calculated bond distances with available experimental values. The calculated distances are also summarized in Figure 3. In the discussions that follow, we refer specifically to quantitative results from the 6-31G* and 6-31G*/MP2 calculations. Bond distances from the STO-3G* basis set usually appear in parentheses. With the few exceptions noted below, all three levels of theory give qualitatively similar conclusions.

Bond Length Comparisons

At the 6-31G* level, the agreement between calculated and experimental bond distances could hardly be better, differences being less than 0.01 Å. Larger differences arise with the STO-3G* basis set; SN bonds in $S_3N_2^+$ (**8**, $^2A_2$) are calculated to be 0.02–0.03 Å longer than experiment (**1**) and the calculated SS distance is too short by 0.1 Å. But even at the STO-3G* level the relative order of calculated distances matches that from experiment for $S_3N_2^+$: NS (equivalent) > NS (unique). Next, compare among themselves the calculated distances for $S_3N_2^{2+}$ (**7**), $S_3N_2^+$ ($^2A_2$, **8**, and $^2B_1$, **9**) and S_3N_2 ($^3B_2$, **10**, and $^1A_1$, **11**). The ab initio calculations support our π-electron-counting rules, giving six electrons to $S_3N_2^{2+}$ and seven electrons to $S_3N_2^+$. In the $^2A_2$ state, $S_3N_2^+$ has a single electron in $2a_2$. This MO has a node that passes through the unique sulfur and between the two equivalent sulfurs. This node of singly occupied $2a_2$ lengthens the SS distance from 2.093 Å in $S_3N_2^{2+}$ (**7**) to 2.135 Å in the $^2A_2$ state of $S_3N_2^+$ (**8**). The $2a_2$ MO is also antibonding between each nitrogen and its adjacent equivalent sulfur, causing this NS (equivalent) bond to lengthen from 1.535 Å in $S_3N_2^{2+}$ to 1.606 Å in **8**. As expected, the $^2B_1$ state of $S_3N_2^{2+}$ (**9**) has higher total energy than the $^2A_2$ state (**8**). The change involves moving an electron from $2a_2$ to $3b_1$. In this process, the electron goes from the $2a_2$ MO that is SS antibonding to the $3b_1$ orbital that is SS bonding, resulting in a significant decrease of the calculated SS bond length. Indeed, the ab initio results show that the SS distance in **9** is even shorter than that in **7**. Both $2a_2$ and $3b_1$ are antibonding between N and the adjacent equivalent sulfur, and both $^2A_2$ and $^2B_1$ states of the radical cation have longer NS (equivalent) bonds than the dication **7**. For the NS (unique) bond, $3b_1$ is antibonding while $2a_2$ is nonbonding. Therefore one expects a longer NS (unique) bond in $^2B_1$ (**9**) than in $^2A_2$ (**8**) as the calculated results show.

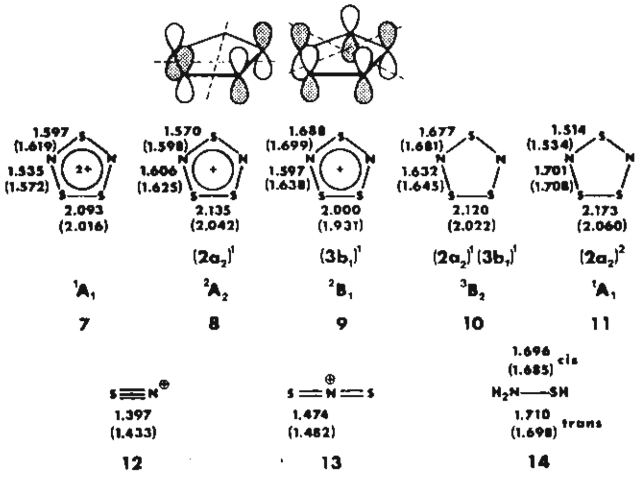

Figure 3. Geometry optimized ab initio SCF MO results at the 6-31G* level (with STO-3G* results in parentheses) for some sulfur–nitrogen species. AO composition diagrams above **8** and **9** show the nodal properties of the singly occupied MO's $2a_2$ and $3b_1$, respectively.

Now consider the hypothetical neutral ring S_3N_2. Although the degeneracy of the 2e″ levels of the homocycle is lost in the heterocycles, the actual splitting between $2a_2$ and $3b_1$ is small (1.0 eV at the 6-31G* level for $S_3N_2^{2+}$). The total energies in Table I show that the open-shell triplet state of ($^3B_2$, **10**, $(2a_2)^1(3b_1)^1$) has lower energy than the closed-shell singlet state ($^1A_1$, **11**, $(2a_2)^2$) for SCF results with STO-3G* and 6-31G* basis sets, but the order of these states is reversed when electron correlation corrections at the MP2 level are added to 6-31G* energies. Next,

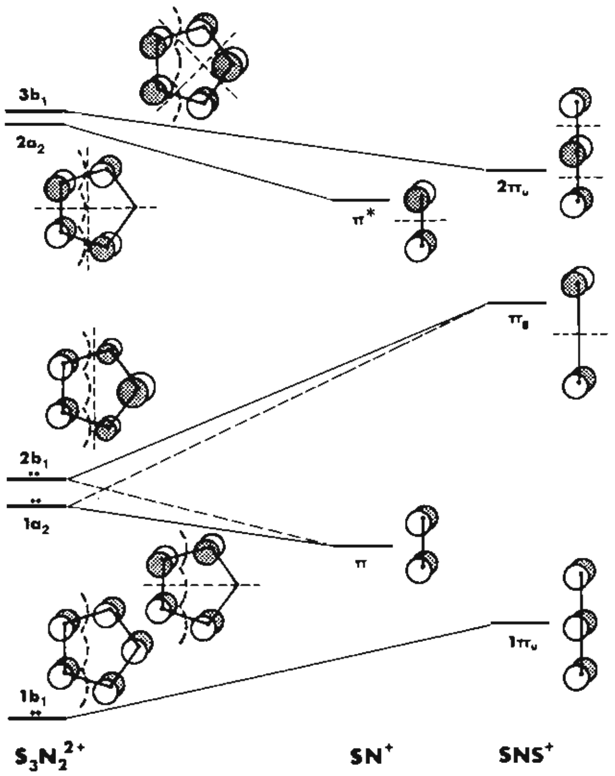

Figure 4. Correlations of the five π MO's for cyclic S_3N_2 with five π MO's for separated diatomic and triatomic fragments. Correlations assume C_s symmetry (all a″). Energy levels are those from extendedd Hückel calculations.

compare the calculated bond distances for closed-shell singlet neutral S_3N_2 ($^1A_1$, **11**) with those for the radical cation ($^2A_2$, **8**). The neutral singlet has an additional electron in $2a_2$, which is antibonding for both SS and NS (equivalent) bonds and gives the neutral singlet longer SS and NS (equivalent) bonds compared to the radical cation ($^2A_2$). Finally, compare calculated bond distances for the open-shell triplet ($^3B_2$, **10**) with those of the radical cation ($^2A_2$, **8**). Addition of an electron to the $3b_1$ level lengthens both NS bonds and shortens the SS bond as anticipated from the nodal character of $3b_1$.

For the NS single bond in H_2NSH, calculations with both basis sets give NS distances less than 0.01 Å shorter than the experimental values, and they reproduce the trend of the experimental results, with NS (trans) longer than NS (cis). At 6-31G* and 6-31G*/MP2 levels the total energy (Table I) of the trans conformer of H_2NSH is slightly lower (less than 1 kcal/mol) than that of the cis conformer, again in agreement with experiment. For the STO-3G* basis set, the cis form is slightly more stable.

Decomposition Processes

The radical cation **1** is stable in solution but the dication **2** dissociates into SN^+ and SNS^+ according to eq 1. That this reaction is spontaneous says that $\Delta G < 0$ and it is likely that ΔH and ΔE are negative as well. The decomposition is one in which numbers of electron pairs are conserved (isogyric),[30] giving some hope that correlation energy errors might approximately cancel in the energy difference between reactants and products. Using the values in Table I to calculate the energy change for eq 1 gives $\Delta E_1 = -120$ (6-31G*/MP2), -95 (6-31G*), and -22 kcal/mol (STO-3G*). Figure 4, based on energy levels from extended Hückel calculations, correlates valence MO's for the dissociation of planar cyclic $S_3N_2^{2+}$ into SN^+ and SNS^+. The highest symmetry that might be maintained during this process is C_s. Crucial to the conclusions to be drawn from Figure 4 is the location of the antibonding MO π^* of the diatomic fragment at lower energy than the antibonding MO $2\pi_u$ of the triatomic fragment; this arrangement is supported by the results of the extended Hückel calculations. $S_3N_2^{2+}$ has 26 valence electrons that occupy 13 MO's. Of these, three are π MO's (a″, antisymmetric with respect to reflection in the plane of the ring) and 10 are σ MO's (a′, symmetric). In SN^+ only one of the occupied MO's (one of the degenerate bonding π MO's) is antisymmetric (a″) with respect to reflection in the common plane of the product fragments SN^+ and SNS^+. The four remaining occupied valence MO's of SN^+ are symmetric (a′) with respect to the plane. SNS^+ has 16 valence electrons in eight MO's. Both bonding and nonbonding degenerate π MO's are fully occupied, and one member of each π set has a″ symmetry. The six remaining occupied valence MO's are symmetric (a′). Thus, three occupied a″ MO's of $S_3N_2^{2+}$ feed electrons into three a″ MO's of SN^+ and SNS^+. Similarly, 10 occupied a′ MO's of $S_3N_2^{2+}$ connect with an equal number of a′ MO's in products SN^+ and SNS^+. The dissociation is symmetry allowed.

It is obvious from the energy levels shown in Figure 4 that sums of orbital energies favor the $S_3N_2^{2+}$ ring rather than the fragments SN^+ and SNS^+, and this observation is confirmed by the sums of energies of σ and π valence orbitals from both extended Hückel and ab initio calculations. However, ab initio total energies favor the fragments compared to the ring. The decomposition of $S_3N_2^{2+}$ is apparently driven by nuclear–nuclear repulsions.

One might have expected $S_3N_2^{2+}$ to yield more symmetric products such as S_2 and NSN^{2+} or S_2^{2+} and NSN, dissociations that follow C_{2v} symmetry. Of the first pair of hypothetical products, S_2 is well-known.[31] The dication NSN^{2+} is apparently unknown although it would be isoelectronic with N_3^+, which has at least been detected spectroscopically.[32,33] N_3^+ is apparently linear and asymmetric, a diradical with only two electrons in the degenerate pair of nonbonding π MO's (π_g, Figure 4).[34-36] NSN^{2+} would probably be the same. The coplanar dissociation of $S_3N_2^{2+}$ into S_2 and NSN^{2+} is symmetry forbidden, in that MO's of reactant do not feed electrons into the appropriate levels for these products.

Of the other pair of possible decomposition products, S_2^{2+} is at least plausible, in isoelectronic analogy with N_2 and SN^+. Indeed, S_2^{2+} may have been produced and subsequently observed spectrophotometrically in the anodic oxidation of elemental sulfur in an $NaCl$–$AlCl_3$ melt at 150 °C.[37] The complementary product NSN is apparently unknown although it would be isoelectronic with CO_2 and even SNS^+. The isomer NNS has been reported,[38] but this species could not be a primary decomposition product of $S_3N_2^{2+}$. The coplanar dissociation

$$S_3N_2^{2+} \rightarrow S_2^{2+} + NSN \tag{2}$$

is symmetry allowed although these symmetrical products appear to be less favorable than the observed and isoelectronic products SN^+ and SNS^+. The calculated energy difference between products and reactants of eq 2 is highly endothermic: $\Delta E_2 = +157$ (6-31G*/MP2), +184 (6-31G*), or +225 kcal/mol (STO-3G*), from energies in Table I. Thus the observed decomposition, eq 1, remains the only feasible process.

The radical cation $S_3N_2^+$ is stable in solution. What prevents it from dissociating into products according to eqs 3 or 4? The

$$S_3N_2^+ \rightarrow SN + SNS^+ \tag{3}$$

$$S_3N_2^+ \rightarrow SN^+ + SNS \tag{4}$$

neutral radical SN has been observed spectroscopically.[39-41] Very

---

(30) Hehre, W. J.; Radom, L.; Schleyer, P. v. R.; Pople, J. A. *Ab Initio Molecular Orbital Theory*; Wiley: New York, 1986; p 276.

(31) Fink, E. H.; Kruse, H.; Ramsay, D. *J. Mol. Spectrosc.* **1986**, *119*, 377.
(32) Lindinger, W. *J. Chem. Phys.* **1976**, *64*, 3720.
(33) Jonkman, H. T.; Michl, J. *J. Am. Chem. Soc.* **1981**, *103*, 733.
(34) Archibald, T. W.; Sabin, J. R. *J. Chem. Phys.* **1971**, *55*, 1821.
(35) Wright, J. *J. Am. Chem. Soc.* **1974**, *96*, 4753.
(36) Venanzi, T. J.; Schulman, J. M. *Mol. Phys.* **1975**, *30*, 281.
(37) Fehrmann, R.; Bjerrum, N. J.; Poulsen, F. W. *Inorg. Chem.* **1978**, *17*, 1195.
(38) Powell, F. X. *Chem. Phys. Lett.* **1975**, *33*, 393.
(39) Zeeman, P. B. *Can. J. Phys.* **1951**, *29*, 174.
(40) Jenouvrier, A.; Pascat, B. *Can. J. Phys.* **1980**, *58*, 1275.

recent microwave studies have revealed the production of the neutral SNS radical,[42] which would be isoelectronic with the highly stable radical ONO. Ab initio SCF MO calculations with configuration interaction predict that SNS is symmetric and bent with an SNS angle of 150° and a barrier of only about 3 kcal/mol to inversion through linear geometry.[43] According to Figure 4, eq 3 is symmetry allowed but eq 4 is forbidden. From the total energies in Table I, both dissociations appear to be endothermic:

$$\Delta E_3 = +21\ (\text{6-31G}^*/\text{MP2}),\ +24\ (\text{6-31G}^*),\quad \text{or } +100\ \text{kcal/mol (STO-3G}^*)$$

$$\Delta E_4 = +36\ (\text{6-31G}^*/\text{MP2}),\ +50\ (\text{6-31G}^*),\quad \text{or } +155\ \text{kcal/mol (STO-3G}^*)$$

Therefore, an extra electron makes $S_3N_2^+$ stable relative to dissociation compared to $S_3N_2^{2+}$.

Conclusions

Geometry optimized ab initio SCF MO calculations with STO-3G* and 6-31G* basis sets confirm that the ground state of $S_3N_2^+$ is $^2A_2$ as has been shown by ESR experiments. The calculated bond distances in $S_3N_2^+$ agree very well with those measured by X-ray crystallography. For the hypothetical neutral heterocycle S_3N_2, our calculations at the SCF level predict that the open-shell configuration $(2a_2)^1(3b_2)^1$ has lower energy than the closed-shell configurations $(2a_2)^2$ and $(3b_1)^2$, but MP2 correlation corrections reverse the order of the $^1A_1$ and $^3B_2$ states. The small splitting between the π levels $2a_2$ and $3b_1$ make this a close call. Optimized ab initio bond distances show differences between $S_3N_2^{2+}$, $S_3N_2^+$, and S_3N_2 in various electronic states that correlate with the qualitative model based on nodal properties of the $2a_2$ and $3b_1$ π MO's. Dissociation of $S_3N_2^{2+}$ into SN^+ and SNS^+ is favored by orbital symmetry and the nature of these fragments. A single electron in the $2a_2$ MO of $S_3N_2^+$ stabilizes this radical cation against dissociation.

Acknowledgment. We are grateful to the National Science Foundation for partial support of this research through Grant No. CHE-9012216 to the University of South Carolina.

---

(41) Matsumura, K.; Kawaguchi, K.; Nagai, K.; Yamada, C.; Hirota, E. *J. Mol. Spectrosc.* **1980**, *84*, 68.
(42) Amano, T.; Amano, T. reported in ref 43.
(43) Yamaguchi, Y.; Xie, Y.; Grev, R.S.; Schaefer, H. F., III *J. Chem. Phys.* **1990**, *92*, 3683.

Contribution from the Institut für anorganische Chemie, Universität Bern, Freiestrasse 3, CH-3000 Bern 9, Switzerland,
and Laboratoire d'Optique Physique, ESPCI, 10, Rue Vauquelin, 75231 Paris Cedex 05, France

Double Excitations of $Ti^{2+}Mn^{2+}$ Spin Clusters in $MgCl_2$, $MnCl_2$, and $MnBr_2$

Markus Herren,[†] Michael A. Aebersold,[†] Bernard Briat,[‡] and Hans U. Güdel*[,†]

Received February 8, 1991

Blue-shifted sidebands on the well-known Mn^{2+} absorptions are observed in the visible absorption and MCD spectra of manganese chloride and bromide doped with Ti^{2+} and of magnesium chloride doped with both Ti^{2+} and Mn^{2+}. These sidebands are assigned to $Ti^{2+}Mn^{2+}$ double excitations of exchange-coupled Ti^{2+}–Mn^{2+} pairs ($MgCl_2$) and $Ti^{2+}(Mn^{2+})_6$ clusters ($MnCl_2$, $MnBr_2$), respectively. The energy differences ΔE of roughly 680 (chlorides) and 600 cm^{-1} (bromide) to the Mn^{2+} absorptions correspond to the trigonal splitting of the Ti^{2+} $^3T_{1g}(O_h)$ ground state. In the $^4A_{1g}{}^4E_g$ (Mn^{2+}) region, the absorption lines are sharp and ΔE in the visible absorption spectrum of $MgCl_2$:Ti^{2+},Mn^{2+} matches the known ground-state splitting of a Ti^{2+}–Mn^{2+} pair in $MgCl_2$. The trigonal ground-state splitting of Ti^{2+} in $MnBr_2$ has not been measured before. The principle of coupling an infrared electronic excitation on one ion with a visible excitation on a neighboring ion should be applicable to many other pairs of ions.

Introduction

Splittings of orbitally degenerate ground states of transition-metal ions in complexes and crystals resulting from low-symmetry ligand-field potentials and spin–orbit coupling are difficult to detect. They are often in the energy range 10–1000 cm^{-1}, which is not easily accessible by experiment. The magnetic susceptibility between 300 and 4 K may provide a rough estimate of the splitting.[1] Among the spectroscopic techniques that have been used to determine ground-state splittings, we mention infrared absorption spectroscopy,[2] electronic Raman spectroscopy,[3,4] and inelastic neutron scattering.[5] The latter two techniques have long been used to determine crystal-field splittings of rare-earth-metal ions in crystals.[6,7] We have recently found that luminescence spectroscopy provides a very accurate picture of the $^3T_{1g}$ ground-state splitting of Ti^{2+} and V^{3+} ions in various ionic lattices.[8,9]

In the present paper, we describe a principle by which a ground-state splitting can be made observable in the visible part of the absorption spectrum. We use Ti^{2+}–Mn^{2+} pairs in $MgCl_2$ and $Ti^{2+}(Mn^{2+})_6$ spin clusters in Ti^{2+}-doped $MnCl_2$ and $MnBr_2$ to illustrate both the principle and the effect. In these species, the Ti^{2+} and Mn^{2+} ions are coupled by exchange interactions. One of the consequences of exchange interactions is the occurrence of cooperative pair or cluster excitations, which have been studied for a long time.[10] The simultaneous excitation of a transition on two neighboring ions can lead to an absorption band at an energy corresponding roughly to the sum of the two single excitations.[11] In many cases, double excitations are observed in pairs of equal ions at twice the energy of single-ion ligand-field excitations.[12] By the same mechanism, two transitions with very different energies can also combine. In the present work, a transition within the energetically split $^3T_{1g}$ ground state of Ti^{2+} is added to a well-known ligand-field transition of Mn^{2+} in the blue spectral region.

The $^3T_{1g}$ (O_h) ground state of Ti^{2+} in the $MgCl_2$ and $MnCl_2$ lattices shows a large trigonal splitting ΔE of the order of 700 cm^{-1} into the components $^3A_{2g}$ and ^3E_g.[8] If a cooperative ab-

---

[*] Author to whom correspondence should be addressed.
[†] Universität Bern.
[‡] ESPCI.

(1) Carlin, R. L. *Magnetochemistry*; Springer-Verlag: Heidelberg, Germany, 1986.
(2) Prinz, G. A. *Physica* **1977**, *89B*, 189.
(3) Clark, R. J. H.; Turtle, P. C. *Chem. Phys. Lett.* **1977**, *51*, 265.
(4) Lockwood, D. J.; Johnstone, I. W. *J. Appl. Phys.* **1982**, *53*, 8169.
(5) Furrer, A.; Wagner, V. *Verh. DPG (VI)* **1981**, *16*, 282.
(6) Amberger, H. D.; Rosenbauer, G. G.; Fischer, R. D. *Mol. Phys.* **1976**, *32*, 1291.
(7) *Proceedings of the Second International Conference on Crystal Field Effects in Metals and Alloys*; Furrer, A., Ed.; Plenum Press: New York, 1977.
(8) Jacobsen, S. M.; Güdel, H. U.; Daul, C. A. *J. Am. Chem. Soc.* **1988**, *110*, 7610.
(9) Reber, C.; Güdel, H. U. *J. Lumin.* **1988**, *42*, 1.
(10) Dexter, D. L. *Phys. Rev.* **1962**, *126*, 1962.
(11) Güdel, H. U. *Comments Inorg. Chem.* **1984**, *3*, 189.
(12) Riesen, H.; Güdel, H. U. *Mol. Phys.* **1987**, *60*, 1221.